Available online at www.sciencedirect.com

ScienceDirect

High Energy Density Physics 3 (2007) 211–217

High Energy Density Physics

www.elsevier.com/locate/hedp

Spectroscopic characterization of ion collisions and trapping at laser-irradiated double-foil targets

O. Renner [a,*], F.B. Rosmej [b], P. Adámek [c], E. Dalimier [d], A. Delserieys [e], E. Krouský [a], J. Limpouch [c], R. Liska [c], D. Riley [e], R. Schott [d]

[a] Institute of Physics, Academy of Sciences CR, Na Slovance 2, 18221 Prague, Czech Republic
[b] CNRS – Université de Provence, PIIM-DPG, Centre de Saint-Jérôme, Marseille, France
[c] Czech Technical University in Prague, Faculty of Nuclear Sciences and Physical Engineering, Prague, Czech Republic
[d] LULI – Université de Paris VI, Paris and École Polytechnique Palaiseau, France
[e] Queens University, Belfast, UK

Available online 25 February 2007

Abstract

Precise X-ray spectroscopic investigation of the colliding plasmas produced at single-side laser-irradiated double-foil Al/Mg targets is reported. The spatially resolved, time-integrated line spectra of the Al Lyα group were measured using a high-dispersion vertical-geometry Johann spectrometer. The X-ray spectra were evaluated with the multilevel collisional-radiative code MARIA. The complex satellite-rich structure observed in the Al Lyα emission indicates a presence of relatively cold dense plasma close to the Al foil surface, hot plasma between both foils, and Al ion trapping close to the Mg foil. An unusual formation of the Al spectra at the Mg foil surface is discussed in terms of interaction of counter-propagating plasmas, in particular trapping, deceleration and thermalization of the Al ions in the colliding plasmas. The qualitative analysis of the observed spectral emission is supported by 2D hydrodynamic modeling and by time-resolved imaging of the expanding plasma. Prospective use of the J-satellite line shifts in diagnosis of colliding laser-produced plasmas is discussed.

PACS: 52.50.Jm; 52.20.Hv; 52.70.La; 32.70.Jz; 52.65.−y

Keywords: Laser-produced colliding plasmas; X-ray spectroscopy; Satellite line emission; Plasma diagnostics; Plasma modeling

1. Introduction

An interest in studying the properties of counter-propagating laser-produced plasmas has been motivated by numerous applications of the phenomena accompanying the plasma collisions. Interpenetrating and stagnating plasmas are frequently found in astrophysics and in laboratory experiments designed to model various astrophysical situations, see Refs. [1,2] and references therein. It is also important for a design of sophisticated targets in indirect drive fusion schemes [3] with different collisional scenarios including interaction between individual shells of fusion pellets and also interactions between the blow-off plasma from the walls of a hohlraum and the capsule. Studying of plasma collisions is fundamental for the optimization of X-ray lasers media [4,5], for the investigation of the energy dissipation and instability evolution in the plasmas [6], thermalization of the counter-streaming plasma plumes [6–8], plasma jets creation [9–11], and formation of quasimolecular structures [12]. Applied problems include the plasma jet interactions with the reactor walls and with the residual gas in the interaction chambers [13], and charge-exchange processes [14].

Hitherto, most of the experiments with the laser-produced colliding plasmas concentrated on the observation and interpretation of phenomena occurring close to the axis of two crossed plasma jets or near the midplane between the

* Corresponding author. Tel.: +420 2 6605 2136; fax: +420 2 8689 0527.
E-mail address: renner@fzu.cz (O. Renner).

1574-1818/$ - see front matter
doi:10.1016/j.hedp.2007.02.036

counter-propagating plasmas. Here we present test-bed experiments on interpenetrating plasmas close to the surfaces of the laser-irradiated double-foil targets. Using X-ray spectroscopic techniques we measured spatially resolved spectra of the H- and He-like aluminum characterizing a distribution of the plasma parameters between inner surfaces of the parallel, closely spaced Al and Mg foils irradiated from the Al side only. We compare the experimental data with the results of simulations based on two-dimensional hydrodynamic and collisional-radiative codes, discuss an unusual formation of the Al Lyα transition and it satellites close to the unirradiated Mg foil surface, and suggest possible diagnostic applications of the observed satellite line shifts.

2. Experiment

The experiment was carried out on the iodine laser system at the PALS Research Center in Prague [15]. As schematically shown in Fig. 1, the double-foil targets consisting of two parallel foils of Al (thickness 0.8 μm) and Mg (thickness 2 μm) with a variable spacing of 200—1000 μm were irradiated at normal incidence with one or two counter-propagating laser beams. The laser beams, delivering 5—200 J of frequency-tripled radiation (0.44 μm) in a pulse length of 0.25—0.3 ns, were focused to a diameter of 80 μm, yielding a maximum intensity of 1×10^{16} W/cm^2 on target. Here we concentrate on evaluation of the experimental data obtained at foils separated by a distance of 360 μm and irradiated from the Al side only with the laser energy of 78 J.

The primary diagnostic was a vertical-geometry Johann spectrometer, VJS, which disperses the radiation in a direction parallel to the axis of the cylindrically bent crystal, i.e., as a function of the vertical divergence angle φ. The VJS provides simultaneously two identical sets of spectra symmetric about the central wavelength λ_0 which facilitates the computational reconstruction of the spectra. Other diagnostics included [16,17] an optical spectroscopy, a pinhole camera (with a slit filtered by 8.5 μm of mylar and 40 nm of Al to suppress energies less than 0.8 keV) coupled to a low-magnification X-ray streak camera with temporal resolution of 2.03 ps/pixel and spatial resolution of 2.9 μm/pixel, and a spherically bent mica crystal X-ray spectrometer.

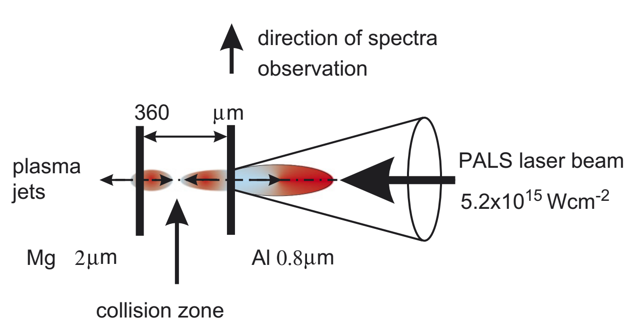

Fig. 1. The scheme of the plasma formation at the laser-irradiated double-foil target.

The VJS was fitted with a crystal of quartz (100) bent to a radius of 76.6 mm and observed the spectrum at an angle of emission $\psi = 0 \pm 0.8°$ to the Al foil surface, the spatial resolution was obtained along the normal to this. The ray-tracing calculations suggest that for the Lyα line of H-like Al, the VJS provides a spectral resolving power about 8000, average linear dispersion of 170 mm/Å, and a collection efficiency two orders of magnitude higher than a comparable flat-crystal scheme. The spatial resolution was limited to 8 μm by the microdensitometer slit width. Due to the extremely high dispersion, the range of the wavelengths $\Delta\lambda$ is $\Delta\lambda/\lambda < 0.03$ allowing coverage of the Al Lyα group including the resonance line and its associated satellites. The time-integrated spectra were recorded on X-ray film Kodak Industrex CX, digitized using the densitometer with an effective slit size 8×80 μm^2 (spatial resolution $\times$ dispersion direction) and recalculated to the linear wavelength and intensity scale by using an algorithm described in Ref. [18]. The reference transition Al XII 2p^2 $^1D_2$—1s2p $^1P_1$, the J-satellite at 7.2759 Å [19], used to calibrate the spectra was defined at the distance of 40 μm from the unirradiated surface of the Al foil.

3. Results and discussion

The reconstructed spectra formed at the single-side irradiated double-foil target are shown in Fig. 2. An outer pair of the strong spectral lines belongs to the Al Lyα doublet, at 7.1709 and 7.1763 Å for the $\alpha_{3/2}$ and $\alpha_{1/2}$ components, respectively, the inner pairs of lines are identified as dielectronic satellites $2l2l' \rightarrow 1s2l'$ with the strongest J-satellite closest to the axis of the spectra symmetry. The enhanced intensity observed close to the Mg foil near the spectra axis is tentatively identified as a combination of the continuum emitted from the foil surface and the Mg He-like 1s^2-1s5p, Heδ, emission, although the survey spectrometer does not observe He-like emission.

When observing the Al Lyα spectral group at the single-foil Al target irradiated by the same laser energy, the emission of the resonance line extends up to several mm above the irradiated front foil surface and about 230 μm below it; the satellite structure can be observed up to approximately 150 μm above and 110 μm below the laser-exploded foil. The effect of the additional Mg foil does not change the character of the

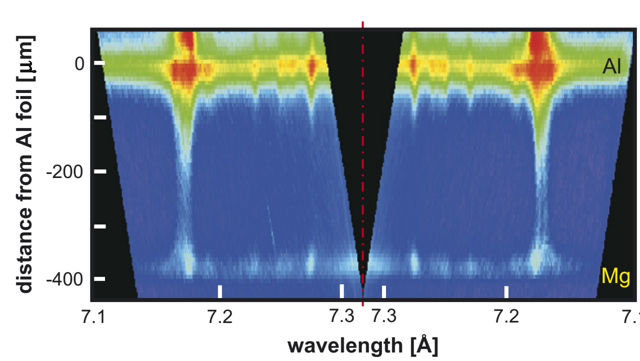

Fig. 2. Reconstructed spatially resolved spectrum of the Al Lyα group observed at single-side laser-irradiated Al/Mg double-foil target.

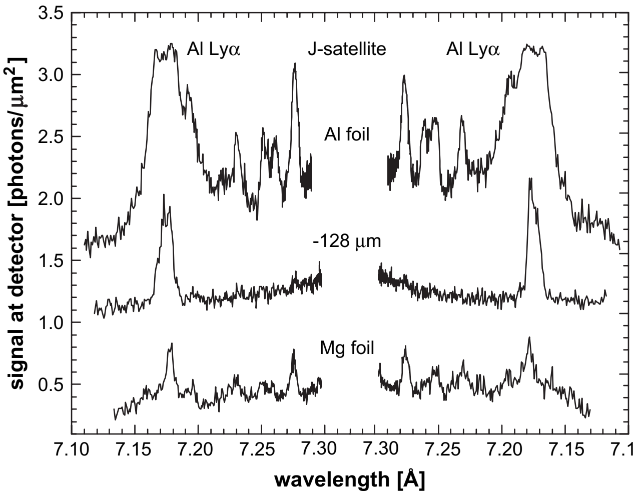

Fig. 3. Spatially resolved spectra observed close to the unirradiated surface of the Al foil, 128 μm below it, and at the Mg foil surface. For clarity, the upper spectral profiles are vertically shifted by +1.0 (−128 μm) and +0.5 photons/μm^2 (at Al foil).

emission above the Al foil, but the extent of the satellite emission below increases to 150 μm. The intensity of the Al Lyα emission below the Al foil approximately doubles, the resonance line is observable throughout the gap between both foils while the Al satellites reappear 50 μm from the Mg foil. The spatial dependence of the intensity distribution among individual spectral components is illustrated in Fig. 3. The satellite-rich structure observed at the unirradiated rear surface of the Al foil gradually reduces to the emission of the Al Lyα only, although at 128 μm below the Al foil a weak J-satellite line can be identified. The satellites reappear near the Mg foil and at the Mg surface the intensity of the J-satellite is comparable with that of the resonance transition.

In order to qualitatively explain this spectra behavior, the plasma evolution was simulated by a 2D hydrocode. Our experimental parameters correspond exactly to the threshold laser intensities $I\lambda^2 \sim 10^{15}\ \mathrm{W\,cm^{-2}\,\mu m^2}$ limiting the use of the Eulerian/Lagrangian fluid codes [6,8,20] and hybrid PIC-fluid models [21], so that an Arbitrary Lagrangian Eulerian (ALE) method [22] was employed. In the ALE method the simulations of the complex mesh is reconstructed and the conserved quantities are remapped on to a smoother grid. Our single-fluid, single-temperature code used 50 cells in a radial direction r, 20 cells for each foil in z-direction, and 20 cells for a void space between the foils. The hydrodynamics was based on a quotidian equation of state (QEOS), classical Spitzer–Harm model for the heat conductivity with a flux limiter set to 20%, and a simple approximation of the laser energy deposition at the critical density surface.

An example of the simulated data is shown in Fig. 4. The plasma evolution characterized by its temperature distribution indicates that the thin upper Al foil burns through before the laser pulse maximum, thus the Al ions are not trapped by the cold Mg foil but collide with the well developed Mg plasma. Then the region of the intense interaction of the Al and Mg ions is situated close to the Mg foil. Time-resolved X-ray imaging validated this as seen in the streak camera record presented in Fig. 5, where the relatively strong emission from the plasma region close to the Mg foil appears before the intensely emitting Al ions reach the Mg surface. The discrepancy in timing of the observed X-ray emission from both plasma plumes, as compared with predictions of the numerical simulations, however, indicates the limited validity of the theoretical model.

The spectroscopic investigation of the plasma conditions was based on a detailed analysis of the Al Lyα group satellite structure performed by using the multilevel, multi-ion stage metastable resolved collisional-radiative code MARIA [23]. The code includes the effects of opacity and covers all Al ground states (nucleus until neutral Al), H-like levels nl with $n=1-4$ and $l=0-3$, He-like levels $1snl$ with $n=1-4$, $l=0-3$, Li-like levels $1s^2nl$ with $n=2-4$, $l=0-3$ and the autoionizing states $2l2l'$, $2l3l'$, $2l4l'$, $1s2l2l'$, $1s2l3l'$ as well as effective dielectronic and radiative recombination rates for all charge states. The variation of the main input parameters (electron density n_e, temperature T_e, the photon path length L, differential plasma motion and line overlapping in

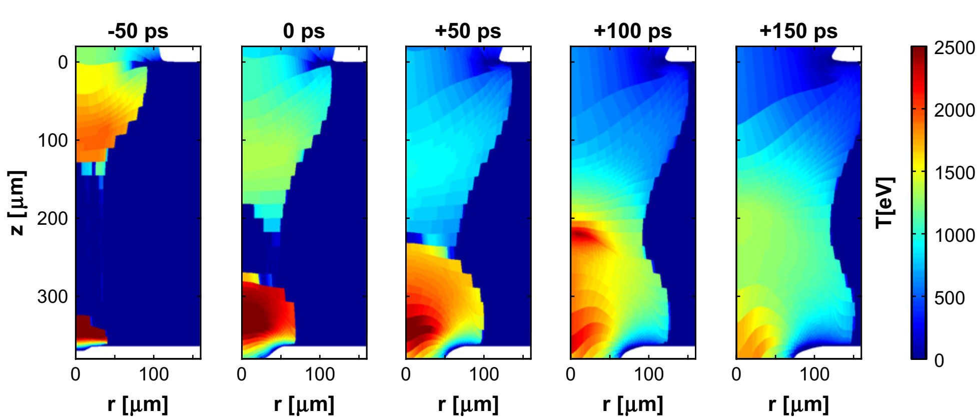

Fig. 4. Evolution of the colliding plasmas simulated by a 2D Arbitrary Lagrangian Eulerian code. The upper foil ($z=0$ μm) is irradiated by a single laser beam from above, the second foil is positioned at the distance of $z=-360$ μm. The timing of the individual temperature frames relates to the laser pulse maximum (0 ps).

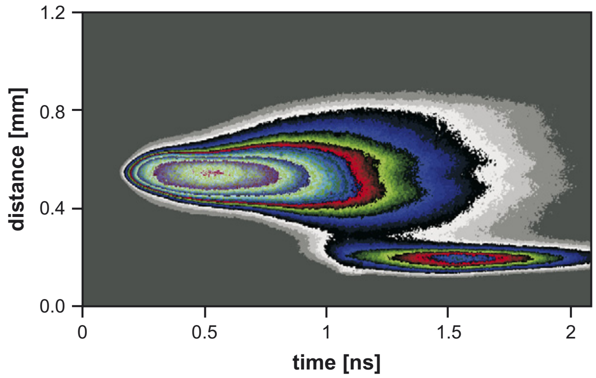

Fig. 5. X-ray streak image of the plasma emission at the double-foil target. The upper plasma plume corresponds to the emission from the laser-irradiated Al foil, the lower plume to the plasma emission close to the Mg foil.

the photon absorption) is seen in modification of the spectral profiles. An example of these calculations, performed for $n_e = 10^{21}$ cm^{-3}, $L = 20$ μm and three temperatures, is shown in Fig. 6, where the satellite transitions are grouped according to their final single excited states. With the decreasing temperature, only the $2l2l'$-satellites attain remarkable intensity whereas Lyα is suppressed considerably. The marked positions of the emission from H- and He-like Mg suggest possible interference of the Al Lyα and ^{1}S-satellite with the Mg He$\varepsilon - \eta$ lines. Although these latter features would have low intensity for spectral analysis they must be included.

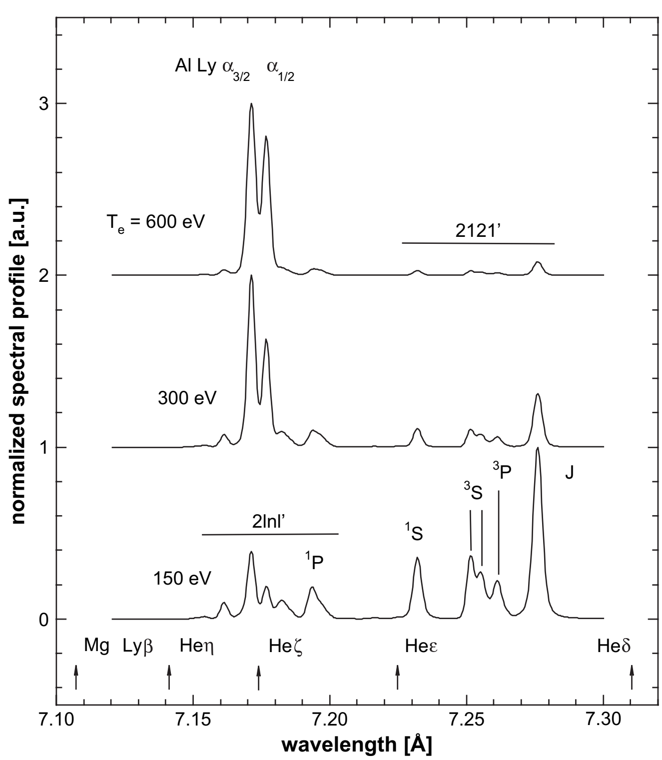

Fig. 6. Theoretical spectra synthesized with the MARIA code demonstrate the intensity redistribution within the Al Lyα group as a function of the electron temperature.

When evaluating the experimental data, the photon path length was considered constant and the electron density and temperature were varied until the best agreement between the experiment and synthesized spectra was achieved. The resulting fits of the left-hand side spectra from Fig. 3 are shown in Fig. 7, where the polynomial background was subtracted and the spectra were normalized. The plasma conditions derived from the Al Lyα group emission observed at the rear surface of the Al foil are $n_e = 3 \times 10^{21}$ cm^{-3}, $T_e = 300$ eV, and $L = 200$ μm. The overall agreement between the synthesized and experimental profiles is good except for the J-satellite line. The lack of a detailed width calculation of this satellite results in its overestimated peak intensity; the integral line intensity, however, is not substantially influenced. Note that we observed in several spectra emitted from single-foil targets the J-satellite emission dominate the Lyα group emission, thus indicating the occurrence of still colder dense plasma at the unirradiated surface of the Al foil. Similar observations were reported earlier in emission from the craters created at the surface of laser-irradiated solid targets only [24].

The Al line emission decreases monotonically with the distance from the Al foil and close to the midplane between both foils, the satellite emission is suppressed and the plasma has electron densities $\sim 3 \times 10^{20}$ cm^{-3} and electron temperatures >700 eV. At ~ 50 μm above the Mg foil surface, the effects resulting from collision and interpenetration of both plasmas

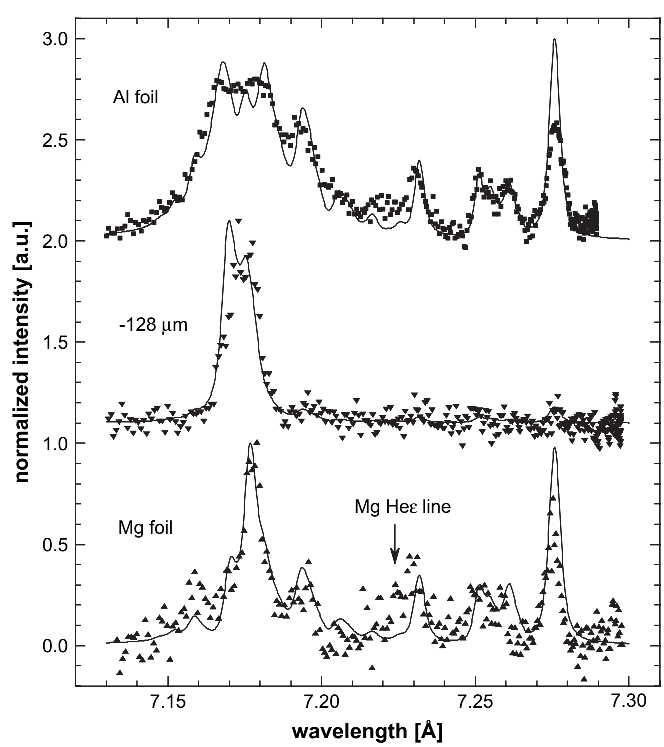

Fig. 7. MARIA code fitting (solid lines) of the experimental left-hand side spectra (points) shown in Fig. 3. The electron temperature increases from 300 eV (inner Al foil surface, $n_e = 3 \times 10^{21}$ cm^{-3}) to above 700 eV (at the distance of −128 μm, $n_e = 3 \times 10^{20}$ cm^{-3}) and then drops again to 220 eV (Mg foil, $n_e \geq 1 \times 10^{21}$ cm^{-3}). The possible overlap of the Mg Heε line with the Al spectrum emitted close to the Mg foil is marked.

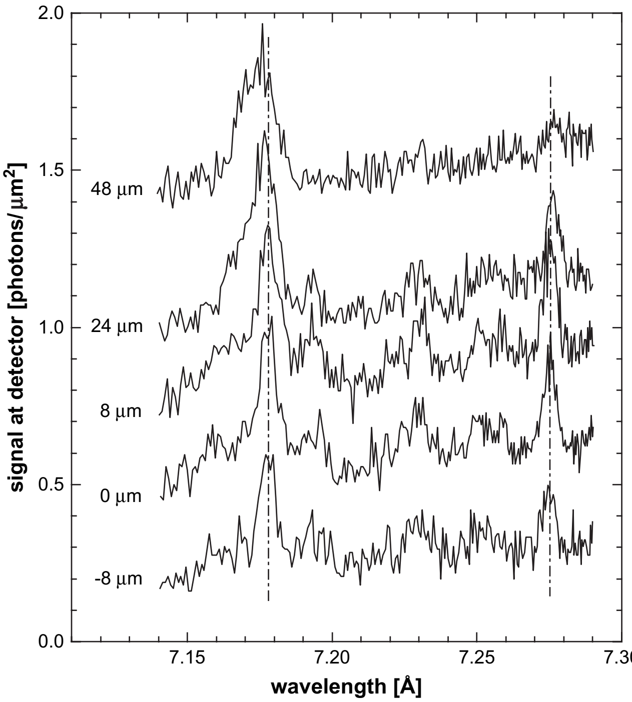

Fig. 8. Evolution of the Al Lyα group emission observed below (at the distance of -8 μm) and above (0–48 μm) the inner surface of the Mg foil. The positions of the Lyα and J-satellite profile centers at the Mg foil are marked by dash–dot lines.

are observed as increased emission of the Al Lyα line and its J-satellite; the whole spectral group can be observed up to about 20 μm below the outside surface of the Mg foil. The plasma conditions at the Mg foil are $n_e \sim 1-3 \times 10^{21}$ cm^{-3}, $T_e \sim 220$ eV, and $L = 500$ μm.

This area close to the Mg foil is of interest for the study of plasma collision and interpenetration phenomena. Spatially resolved spectral scans of the Al Lyα group emission presented in Fig. 8 display several characteristic features: broadening and shift of the resonance line, and variable profiles and positions of the individual satellite components as a function of the distance from the Mg foil surface. The integrated intensities and FWHM widths of the resonance line shown in Fig. 9a provide qualitative information about the density and ion temperature of the colliding plasmas. Assuming that the integrated intensity is proportional to the partial density of the relevant ions, then the Al ion population attains its maximum between 40 and 60 μm above the Mg foil. Fig. 9a also indicates that the FWHM width of the Al Lyα line peaks at the distance of 30–50 μm from the Mg foil. The increase in the line width can be ascribed partially to the Doppler broadening due to the plasma thermalization. Both these parameters are consistent with a region of density buildup and ion heating, i.e., the region where collision and stagnation of the Al and Mg plasmas occurs. On the other hand, the presence of the Al emission near and below the Mg foil provides clear evidence of the plasma interpenetration.

The distinct blue shift of the resonance line with the increasing distance of the emitting region from the Mg foil (shown in Fig. 9b) is ascribed to a combination of the plasma parameters variation, radiative transfer effects of the optically thick line and phenomena connected with the satellite formation, quasi-continuum and potentially the Mg Heζ emission close to the Mg foil surface (cf. Fig. 6). In contrast, the J-satellite position shifts with the increasing distance from the Mg foil (the J-satellite could be observed up to the distance of 50 μm from the foil, then it merged with continuum) almost monotonically to the red whereas its FWHM value 5.3 mÅ remains constant within the experimental error of 1.0 mÅ. This observed shift of the optically thin J-satellite should only be correlated with the variation of the macroscopic plasma parameters derived from the detailed interpretation of the observed spectra.

Here we shall confine ourselves to a discussion of two principal mechanisms capable of explaining the measured J-satellite shift. The first one refers to the velocity distribution of the Al ions in the expanding plasma. Simulations suggest that the Al ions streaming towards the Mg foil are accelerated to velocities above 1×10^8 cm/s at distances as short as 100 μm from the Al foil. When arriving at the Mg foil, they collide with the counter-propagating plasma and decelerate. The gradual ion stopping manifests itself via the Doppler effect. Assuming a complete stopping of the Al ions within the region where the J-satellite is observed at the Mg foil, their overall blue shift

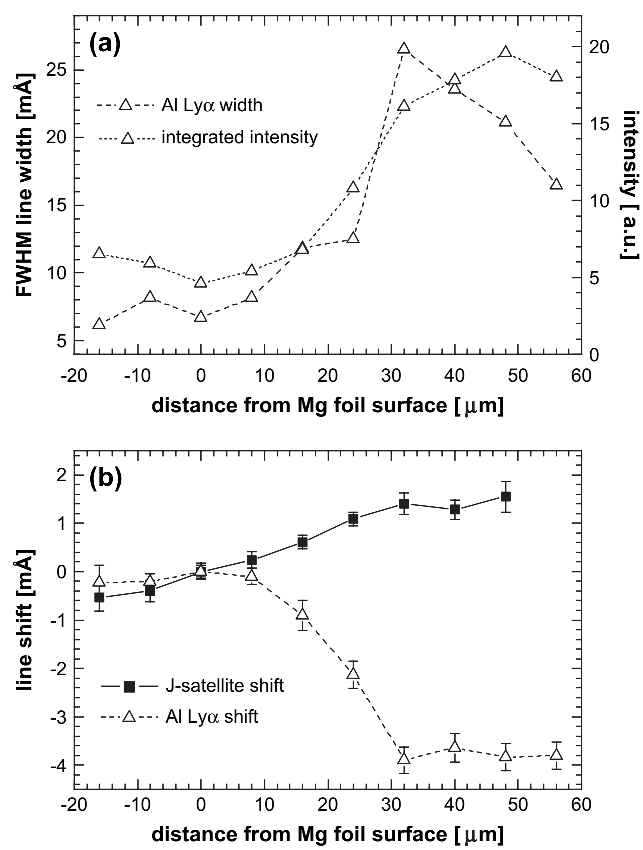

Fig. 9. Integrated intensities and FWHM widths of the Al Lyα emission (a) and shifts of the J-satellite and the resonance line (b) as a function of the distance from the Mg foil surface.

with the decreasing distance from the second foil (until the stagnation behind the original Mg surface) should be smaller or at the level of 0.5 mÅ at our experimental conditions. Obviously, the ion deceleration cannot explain the total shift observed, though contributing to it considerably.

The second possible mechanism is the plasma-induced shifts of the spectral lines. In analogy to the theory and experimental observations of the resonance line transitions (for a survey Ref. [25]), we can expect red shifts of the satellites with the increasing plasma density, i.e., up to about 50 μm from the Mg foil. The combination of both of these mechanisms might fully account for the observed shifts of the J-satellite.

The complex theory of the satellite line shifts has not yet been studied and verified due to a lack of reliable experimental data; however, the experiments reported that the capability to perform the measure now exists. When the theory of the satellite shifts is proved, the observations of the satellite line shifts might provide a very efficient tool for diagnosis of the cold dense plasma, particularly with respect to a moderate optical depth of the satellite transitions.

4. Conclusion

We report X-ray spectroscopic investigation of colliding plasmas produced at single-side laser-irradiated double-foil Al/Mg targets. Time-integrated spectra of the Al Lyα group measured with high spectral and spatial resolution characterize a distribution of the plasma parameters between inner surfaces of the target foils. The detailed analysis of the complex satellite structure in the Al Lyα group based on a multilevel collisional-radiative code MARIA indicates the presence of the relatively cold plasma close to the Al foil surface, occurrence of the hot plasma between both foils, and Al ions trapping close to the Mg foil. An unusual formation of the Al spectra at the Mg foil surface is qualitatively correlated with the plasma-induced line shifts, deceleration of the Al ions close to the Mg foil and thermalization of the colliding plasmas. Prospective use of the observed J-satellite line shifts in diagnosis of cold dense plasma is suggested. To conclude, these precise X-ray data measured under well-defined conditions of the plasma production provide the experimental capability required for testing various theoretical models and for development of novel methods for diagnosis of cold dense plasmas.

Acknowledgments

This research was performed within the EU LASERLAB Program, contract PALS No. 1080, partially funded by the Czech Science Foundation under grant No. 202/06/0801 and by the Czech Ministry of Education under project MSM 6840770022.

References

[1] B.A. Remington, D. Arnett, R.P. Drake, H. Takabe, A review of astrophysics experiments on intense lasers, Phys. Plasmas 7 (2000) 1641.

[2] L.O. Silva, R.A. Fonseca, J.W. Tonge, J.M. Dawson, W.B. Mori, M.V. Medvedev, Interpenetrating plasma shells: near-equipartition magnetic field generation and nonthermal particle acceleration, Astrophysical J. 596 (2003) L121.

[3] T.R. Dittrich, S.W. Haan, M.M. Marinak, S.M. Pollaine, D.E. Hinkel, D.H. Munro, C.P. Verdon, G.L. Strobel, R. McEachern, R.C. Cook, C.C. Roberts, D.C. Wilson, P.A. Bradley, L.R. Foreman, W.S. Varnum, Review of indirect-drive ignition design options for the National Ignition Facility, Phys. Plasmas 6 (1999) 2164.

[4] T. Boehly, B. Yaakobi, D. Shvarts, D. Meyerhofer, P. Audebert, J. Wang, M. Russotto, B. Boswell, R. Epstein, R.S. Craxton, J.M. Soures, X-ray laser experiments using double-foil nickel targets, Appl. Phys. B 50 (1990) 165.

[5] R.W. Clark, J. Davis, A.L. Velikovich, K.G. Whitney, X-ray lasing in colliding plasmas, Phys. Plasmas 4 (1997) 3718.

[6] R.L. Berger, J.R. Albritton, C.J. Randall, E.A. Williams, W.L. Kruer, A.B. Langdon, C.J. Hanna, Stopping and thermalization of interpenetrating plasma streams, Phys. Fluids B 3 (1991) 3.

[7] O. Rancu, P. Renaudin, C. Chenais-Popovics, H. Kawagashi, J.-C. Gauthier, M. Dirksmöller, T. Missalla, I. Uschmann, E. Förster, O. Larroche, O. Peyrusse, O. Renner, E. Krouský, H. Pépin, T. Shepard, Experimental evidence of interpenetration and high ion temperature in colliding plasmas, Phys. Rev. Lett. 75 (1995) 3845.

[8] C. Chenais-Popovics, P. Renaudin, O. Rancu, F. Gilleron, J.-C. Gauthier, O. Larroche, O. Peyrusse, M. Dirksmöller, P. Sondhauss, T. Missalla, I. Uschmann, E. Förster, O. Renner, E. Krouský, Kinetic to thermal energy transfer and interpenetration in the collision of laser-produced plasmas, Phys. Plasmas 4 (1997) 190.

[9] D.R. Farley, K.G. Estabrook, S.G. Glendinning, S.H. Glenzer, B.A. Remington, K. Shigemori, J.M. Stone, R.J. Wallace, G.B. Zimmerman, J.A. Harte, Radiative jet experiments of astrophysical interest using intense lasers, Phys. Rev. Lett. 83 (1999) 1982.

[10] T. Atwee, H.-J. Kunze, Spectroscopic investigation of two equal colliding plasma plumes of boron nitride, J. Phys. D: Appl. Phys. 35 (2002) 524.

[11] A. Kasperczuk, T. Pisarczyk, S. Borodziuk, J. Ullschmied, E. Krousky, K. Masek, K. Rohlena, J. Skala, H. Hora, Stable dense plasma jets produced at laser power densities around 10^{14} W/cm^2, Phys. Plasmas 13 (2006) 062704.

[12] E. Oks, E. Leboucher-Dalimier, Extrema in transition energies resulting not in satellites but in dips within spectral lines, Phys. Rev. E 62 (2000) R3067.

[13] F.B. Rosmej, R. Stamm, V.S. Lisitsa, Convergent coupling of helium to the H/D background in magnetically confined plasmas, Europhys. Lett. 73 (2006) 342.

[14] F.B. Rosmej, H.R. Griem, R.C. Elton, V.L. Jacobs, J.A. Cobble, A.Ya. Faenov, T.A. Pikuz, M. Geissel, D.H.H. Hoffmann, W. Süss, D.B. Uskov, V.P. Shevelko, R.C. Mancini, Charge-exchange-induced two-electron satellite transitions from autoionizing levels in dense plasmas, Phys. Rev. E 66 (2002) 056402.

[15] K. Jungwirth, A. Cejnarova, L. Juha, B. Kralikova, J. Krasa, E. Krousky, P. Krupickova, L. Laska, K. Masek, T. Mocek, M. Pfeifer, A. Präg, O. Renner, K. Rohlena, B. Rus, J. Skala, P. Straka, J. Ullschmied, The Prague Asterix laser system, Phys. Plasmas 8 (2001) 2495.

[16] F.B. Rosmej, A. Delserieys, E.H. Guedda, L. Godberg-Mouret, R. Schott, E. Dalimier, D. Riley, O. Renner, E. Krousky, Investigation of optical transitions of highly charged ions in high density laser produced plasmas at PALS, Europhys. Conf. Abstr. 301 (2006) P-5.034

[17] F.B. Rosmej, V.S. Lisitsa, R. Schott, E. Dalimier, D. Riley, A. Delserieys, O. Renner, E. Krousky, Charge exchange driven X-ray emission from highly ionized plasma jets, Europhys. Lett. 76 (2006) 815.

[18] O. Renner, T. Missalla, P. Sondhauss, E. Krousky, E. Förster, C. Chenais-Popovics, O. Rancu, High-luminosity, high-resolution X-ray spectroscopy of laser-produced plasma by vertical-geometry Johann spectrometer, Rev. Sci. Instrum. 68 (1997) 2393.

[19] NIST Atomic Spectra Database, <http://physics.nist.gov/PhysRefData/ASD/index.html>.

[20] P.W. Rambo, J. Denavit, Interpenetration and ion separation in colliding plasmas, Phys. Plasmas 1 (1994) 4050.

[21] R.G. Evans, Modelling short pulse, high intensity laser plasma interactions, High Energy Density Phys. 2 (2006) 35.
[22] M. Kucharik, J. Limpouch, R. Liska, Laser plasma simulations by Arbitrary Lagrangian Eulerian method, J. Phys. IV France 133 (2006) 167.
[23] F.B. Rosmej, Hot electron X-ray diagnostics, J. Phys. B: At. Mol. Opt. Phys. 30 (1997) L819.
[24] O. Renner, F.B. Rosmej, E. Krousky, P. Sondhauss, M.P. Kalachnikov, P.V. Nickles, I. Uschmann, E. Förster, Overcritical density plasma diagnosis inside the laser-produced craters, Appl. Phys. Lett. 79 (2001) 177.
[25] O. Renner, P. Adámek, P. Angelo, E. Dalimier, E. Förster, E. Krousky, F.B. Rosmej, R. Schott, Spectral line decomposition and frequency shifts in Al Heα group emission from laser produced plasmas, J. Quant. Spectrosc. Radiat. Transfer 99 (2006) 523.